Spontaneous Rotational Inversion in Phycomyces

Alain Goriely
OCCAM, Mathematical Institute, University of Oxford, Oxford OX1 3LB, United Kingdom

Michael Tabor
Program in Applied Mathematics, University of Arizona, Tucson, Arizona 85721, USA
(Received 17 January 2011; published 31 March 2011)

The filamentary fungus *Phycomyces blakesleeanus* undergoes a series of remarkable transitions during aerial growth. During what is known as the stage IV growth phase, the fungus extends while rotating in a counterclockwise manner when viewed from above (stage IVa) and then, while continuing to grow, spontaneously reverses to a clockwise rotation (stage IVb). This phase lasts for 24–48 h and is sometimes followed by yet another reversal (stage IVc) before the overall growth ends. Here, we propose a continuum mechanical model of this entire process using nonlinear, anisotropic, elasticity and show how helical anisotropy associated with the cell wall structure can induce spontaneous rotation and, under appropriate circumstances, the observed reversal of rotational handedness.

DOI: 10.1103/PhysRevLett.106.138103 PACS numbers: 87.10.Pq, 46.70.Hg, 87.19.lx, 87.19.rd

Phycomyces blakesleeanus is the most studied phycomyces, a genus of fungi first reported in the early 19th century and described at length by the Belgian biologist and cleric Jean-Baptiste Carnoy in 1870 [1]. After a complex reproductive cycle, this fungus emerges as a strikingly large, single-celled, aerial hypha—known as the sporangiophore—reaching sizes of up to 10 cm long (see Fig. 1). The organism, its rotating growth phases, and remarkable tropic responses to various external stimuli have long been a source of fascination to biologists and biophysicists alike [2–6].

Helical growth is the rotation of a structure as it extends axially and is observed in many different tubular structures across the plant kingdom [7]. However, it is not known whether this type of growth serves a biological function or provides some mechanical advantage (as hypothesized in the spiral grain of trees [8,9]). Nevertheless, elucidating the physical processes that lead to helical growth provides insights into the fundamental problem of relating cell wall structure to growth and form in plants. The physical explanation for helical growth is based on the intuitive notion that a cylinder with a helically structured (cell) wall, under axial stress due to turgor pressure, should unwind in the absence of an external axial moment. Hence, helical growth can be viewed as the macroscopic mechanical consequence of cell wall anisotropy. We refer to right-handed growth when a point on top of the cylinder, viewed from above, turns counterclockwise during extension and left-handed growth when the same point turns clockwise.

Similar to other systems exhibiting helical growth, the cell wall of the cylindrically structured sporangiophore of *Phycomyces blakesleeanus* is anisotropic, essentially composed of chitin microfibrils embedded in an elastic matrix of amorphous material made out of chitosan and chitin [10,11]. After an initial aerial growth phase (stage I) and the development of the sporangium (stages II and III), axial growth resumes in stage IV. A remarkable behavior is then observed [12]: In stage IVa, right-handed growth takes place for approximately 1 h; this is followed by stage IVb in which left-handed growth is observed that can last up to 48 h. A further rotational inversion (stage IVc) has also been reported by some authors [13]. In a series of experimental and theoretical papers, Ortega, Gamow, and co-workers have presented a geometric explanation for the rotation in stage IVb based on the reorientation of the microfibrils during growth [14,15]. They also suggested that the inversion of rotation may be due to a

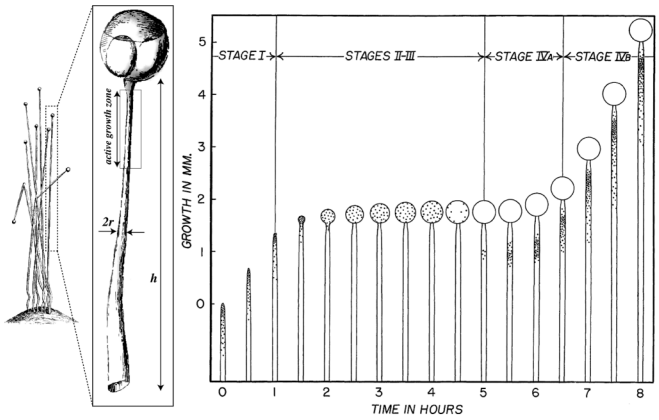

FIG. 1. Left: The fungus *Phycomyces blakesleeanus* as drawn by Carnoy [1]. The spherical dome on top of the tube is the sporangium that contains the spores that are disseminated on completion of the life cycle. Right: The 4 stages of growth for the aerial hypha. In stage IV helical growth reversal is observed: Stage IVa exhibits right-handed growth, and stage IVb presents left-handed growth. Stage IVb continues for up to 2 days when the organisms can reach up to 10 cm in height (reproduced from Ref. [12]).

so-called ''microfibril slippage'' effect, but they did not further elaborate on the mechanics of this process.

Here we present a mechanical model for the rotational reversals observed in stages IVa, IVb, and IVc. We view the sporangiophore as a growing, fiber-reinforced, elastic structure and include a dynamical remodeling and deposition of the fibers. Our basic assumption is that new fibers are deposited in a stress-free state along the direction of existing fibers. The fiber angle starts close to the horizontal direction in a right-handed orientation, and the growth zone increases to its asymptotic size. The rotation of the tube is then simply obtained from the mechanical balance that results from the extension of an anisotropic elastic tube under pressure in the absence of an end moment. Strikingly, the model predicts that under extension a fiber will always tend to align in the axial direction but that the tube can either rotate clockwise or counterclockwise depending on the angle of the fibers and their state of stress. Within this model, the initial right-handed growth is shown to be a transient phenomenon that disappears when the growth zone is sufficiently extended. Once the growth zone is fully established, a regular left-handed growth persists with constant rotation up to a point when the growth zone starts retracting and a further inversion is possible, again as a short transient phenomenon.

The length and time scales in stages IVa and IVb are as follows. A typical radius of the sporangiophore is $l = 50\ \mu$m, and we will use this radius (assumed to be constant throughout these phases) as the length scale. The wall thickness is $l/83$. The growth zone, which is the zone immediately below the sporangium where new cell wall material is added, extends to a size $h \sim 60l$. A typical sporangiophore length is $3\text{–}4 \times 10^3 l$. In stage IVb, the typical axial velocity is a constant $v_z = 60l/\mathrm{h}$, that is, a doubling time of about 1 h for the size of the growth zone. This is accompanied by an angular rotation in stage IVb of approximately $4\pi/\mathrm{h}$ for a duration of 24–48 h. In contrast, stage IVa lasts about 1 h.

We model the sporangiophore as an anisotropic, elastic, incompressible tube with two families of embedded fibers. The first family of fibers is in the hoop direction and provides the cylinder with sufficiently strong radial reinforcement such that under pressure the radius is constant and expansion is confined to a pure extension along the axis. The second family of fibers winds helically (right-handed [16]) around the axis and induces a rotation of the cylinder under extension. The presence of the hoop fibers together with the relative thinness of the wall compared to the radius are used to justify the modeling assumptions that there is no variation (strain or stress) in the radial direction and that the tube radius is constant. Also, since the growth zone is much larger than the radius, we neglect gradient effects in the axial direction.

We consider finite deformations in which the cylinder is allowed to grow, rotate around its axis, and elongate axially while remaining cylindrical. Thus, in cylindrical coordinates with the z axis corresponding to the vertical axis of growth, the rotation is $\theta = \Theta + \tau\zeta Z$, where τ is the torsion, and the axial stretch is $\zeta = z/Z$ (here uppercase symbols correspond to the reference configuration before pressure is applied). The material response is specified by the standard reinforcing model [17] with the simplest possible dependence for its isotropic and anisotropic parts $W(I_1, I_4) = \mu_1/2(I_1 - 3) + \mu_4/4(I_4 - \nu^2)^2$, where the Cauchy-Green deformation tensor invariants are $I_1 = \zeta^2\tau^2 + \zeta^2 + 1/\zeta^2 + 1$, $I_4 = \zeta \sin\Phi[\zeta(\tau^2 + 1)\sin\Phi + 2\tau\cos\Phi] + \cos^2\Phi$. The angle Φ denotes the orientation of the fibers with respect to the horizontal plane in the reference configuration, and ν is the precompression of the fibers in the initial configuration. The anisotropic contribution to the hoop stress is proportional to $(I_4 - \nu^2)$. Since $I_4 = 1$ in an unstressed configuration , the case $\nu > 1$ results in a negative, i.e., compressive, stress. It is straightforward to show that the fiber orientation ϕ in the current configuration is

$$\phi = \arctan\left(\frac{\zeta \sin\Phi}{\cos\Phi + \zeta\tau \sin\Phi}\right), \tag{1}$$

where we have assumed a thin-walled cylinder of constant (unit) radius.

We first consider a static model and assume that our tube is uniform with height H and a fixed fiber angle with a right-handed helical configuration $0 < \Phi < \pi/2$. We then subject it to an internal pressure leading to a given extension ζ that we use to parameterize the internal load. From the strain-energy function, we compute the Cauchy stress tensor $\mathbf{T}$ and verify that it satisfies identically the equilibrium equations (without body force). Since no axial moment is applied on the surface of the tube, the boundary condition is simply $T_{\theta z} = 0$, where

$$T_{\theta z} = \mu_1\zeta^2\tau + \zeta\mu_4 \sin\Phi(\zeta\tau\sin\Phi + \cos\Phi) \times \{\zeta \sin\Phi[\zeta(\tau^2 + 1)\sin\Phi + 2\tau\cos\Phi] + \cos^2\Phi - \nu^2\},$$

which leads to a cubic equation for τ for given values of Φ, ν, ζ, and the ratio $\mu = \mu_4/\mu_1$. This is the torsion needed to relax the torsional stress in the tube induced by the anisotropy. Some of these solutions are shown in Fig. 2.

In the absence of precompressed fibers ($\nu = 1$), we see that the twist τ is always negative; i.e., the top of tube will rotate clockwise by an angle $\Theta = \tau h = \tau\zeta H$ leading to the appearance of left-handed growth. The effect of precompression in the fibers is quite remarkable and nonintuitive. Even for small levels of precompression (e.g., $\nu = 1.05$), at small fiber angles, the cylinder will rotate counterclockwise as shown in Fig. 2. The critical fiber angle Φ_c at which there is no rotation is given by $\Phi_c = \arccos[\sqrt{(\zeta^2 - \nu^2)/(\zeta^2 - 1)}]$ and clearly requires $\zeta > \nu$. The inversion occurs when fibers go from compression to tension, since the critical angle corresponds to the point

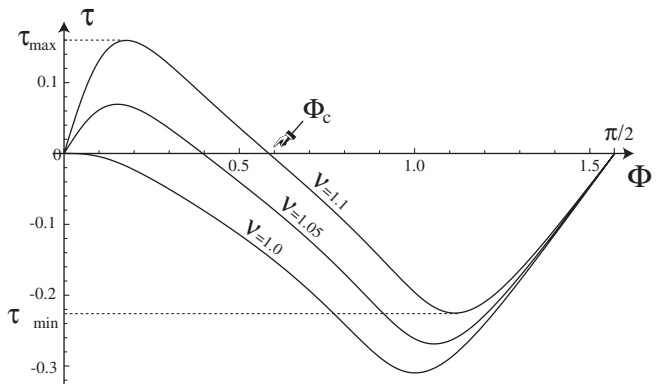

FIG. 2. Effect of fiber precompression on torsion τ as a function of the fiber angle Φ (the behaviors illustrated in Figs. 2–4 are all for $\mu = 5$, $\zeta = 1.4$ but are robust to changes in the parameter values).

$I_4 = \nu^2$. In the absence of precompression, the cylinder rotates clockwise. Despite the torsional inversion, the fiber orientation in the current configuration is always greater than the orientation in the reference configuration (see Fig. 3).

From the expression for $T_{\theta z}$ it is possible to obtain a lower bound $\tau_{\min}$ and a lower upper bound $\tau_{\max}$ for the torsion in the limit of stiff fibers $\mu \gg 1$, namely,

$$\tau_{\min} = -\sqrt{(\zeta^2 - \nu^2)}/\nu\zeta, \qquad \tau_{\max} = \sqrt{\mu}(\nu - 1)\nu/\zeta. \quad (2)$$

We have shown that a fiber-reinforced elastic tube with right-handed helical fibers can rotate clockwise or counterclockwise depending on the initial angle, axial extension, and initial stress in the fiber. We use this key result to develop a model of growing phycomyces in which new fibers are continuously laid down in an evolving growth zone at the top of the sporangiophore. Our key assumptions are that (i) new fibers are laid down stress-free along the direction of fibers in the current configuration and (ii) the growth zone extends linearly in time to a size h within the first 2 h. A crucial concept is that the current configuration at a given time step becomes the reference configuration for the next time step. The overall growth process can now be explained as follows. Consider a material point in the cell wall. Initially, fibers are laid down at some small angle Φ_0 with $\nu_0 = 1$ at the top of the growth zone. The extension (due to the turgor pressure) and the rotation (due to the relaxation of the torsional stress) of the cylinder result in the fibers reorienting to an angle ϕ_1. As growth proceeds, the material point moves downward with respect to the top of the growth zone, and new fibers at the same material point are laid down with angle $\Phi_1 = \phi_1$ and zero stress. This material point now has a mixture of fibers with angles Φ_0 and Φ_1. The effective stress in the fibers in this new reference configuration (at this material point) is thus a combination of fibers with precompressions ν_0 and ν_1. A continuous model of this process is given by

$$\frac{\partial \Phi}{\partial t} = \kappa_1(\phi - \Phi), \qquad \frac{\partial \nu}{\partial t} = \kappa_2(\zeta - \nu)\sin\Phi, \quad (3)$$

where Φ, ϕ, ν, and ζ are all evaluated at Z, the distance from the top of the sporangiophore of a material point in the reference configuration. Following the property of the angle $\phi = \phi(\Phi)$ given above, we have $\Phi(t) \to \pi/2$ and $\nu(t) \to \zeta$ as $t \to \infty$. The time constant $1/\kappa_1$ is fitted so that when a material point leaves the growth zone the associated fiber is oriented along the axis, i.e., $\Phi(1) \approx \pi/2$, and similarly $1/\kappa_2$ is fitted to match the time for rotational inversion. As an example of the dynamics generated by this system (coupled to the equations for ϕ and τ), we show in Fig. 4 the evolution of τ, Φ, and ν as a function of time.

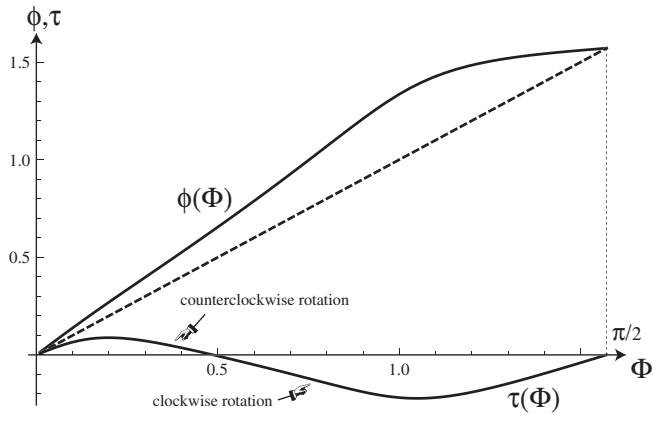

FIG. 3. Fiber orientation ϕ in the current configuration as a function of Φ, and the corresponding plot of $\tau(\Phi)$. The dashed diagonal line corresponds to $\phi = \Phi$.

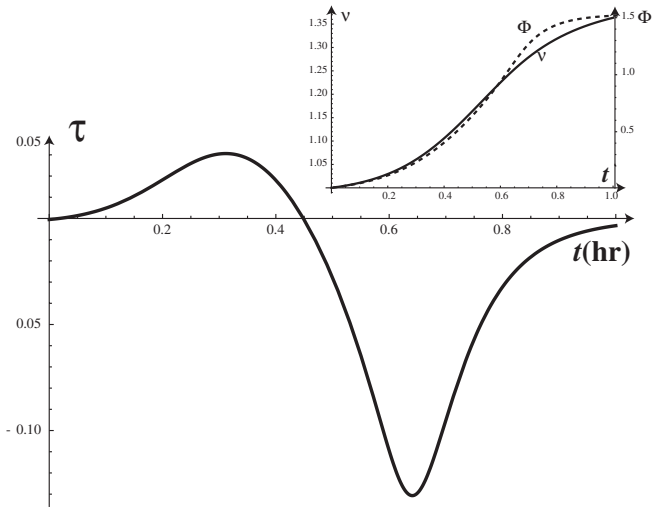

FIG. 4. Dynamic of τ, ν, and Φ for a given material point as a function of time ($\kappa_1 = 16\ \mathrm{h}^{-1}$, $\kappa_2 = 4\ \mathrm{h}^{-1}$. While this process takes place, the material point at $t = 0$ starts on top of the growth zone and is convected downward (with respect to a reference frame moving with the top of the growth zone).

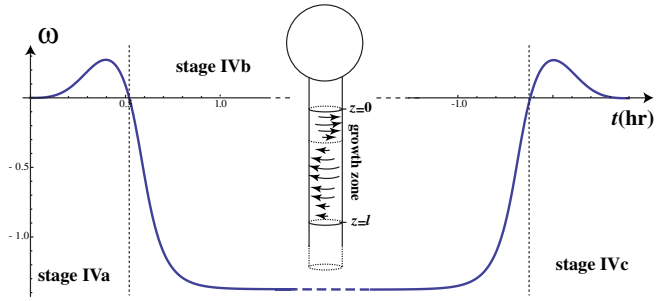

FIG. 5 (color online). Rotational velocity (in units of radians per unit time t_r) of the sporangiophore as a function of time. The time -1 on the right side of the time axis refers to 1 h before the end of growth, i.e., the time in this simulation at which the growth zone starts to retract.

Each time the tube extends and twists as an elastic response to the extensional and torsional stresses, there is an evolution of the reference configuration due to the deposition of new fibers and other wall building materials. The net result is a continuous remodeling of the cell wall leading to an irreversible growth of the tube. The rotation of a small disk of height ΔZ at point Z measured from the top of the growth zone with fiber angle Φ and precompression ν (in the reference configuration) is $\Delta\theta = \tau[\Phi(Z), \nu(Z)]\Delta z = \tau\zeta\Delta Z$. Thus the total rotational velocity, ω, can be estimated as

$$\omega = t_r^{-1}\int_0^H \tau[\Phi(Z), \nu(Z)]\zeta dZ, \tag{4}$$

where t_r is a characteristic time scale corresponding to the remodeling time of the reference configuration.

We can now use our model for the evolution of the fiber angle and the fiber precompression to compute the rotational dynamics of our growing cylinder. We assume that the growth zone extends linearly in time with a constant velocity v_z up to a length $h = H\zeta$ (corresponding to the end of stage IVa). Then the length of the growth zone remains stationary (stage IVb) and the tube extends, while rotating at a constant rate, until the growth zone retracts resulting in another inversion (stage IVc) as shown in Fig. 5.

Initially, before the growth zone is fully established, only the fibers in the top part of the zone play a role and the net rotation is counterclockwise leading to right-handed growth (stage IVa). Once the growth zone is fully established, the observed rotation of the sporangium is determined by the integral over the entire zone, hence leading to a left-handed spiral (stage IVb). Interestingly, the model predicts that at any given time there are individual material points in the growth zone turning both counterclockwise (top of the growth zone) and clockwise (bottom). The integrated effect of these rotations depends on the extent of the growth zone. This is entirely consistent with the detailed observations of Ref. [18] on the rotation of individual points in the growth zone. Estimates of the rotational velocity depend on the choice of the time scale t_r. From Fig. 5, we see that in stage IVb $|\omega| \sim 1.5$, and for the range of t_r, $1/\kappa_1 \leq t_r \leq 1/\kappa_2$, one finds the corresponding range of 1–4 turns/h. This is qualitatively consistent with the observed 2 turns/h.

The model proposed here relies on two simple fundamental assumptions: First, new fibers are laid down along the direction of existing fibers; second, new fibers are laid down in a stress-free state. The rotational inversion is then a direct consequence of the response of a tubular, fiber-reinforced, morphoelastic material, namely, a material that responds elastically on short time scales (relieving torsional stress by rotation of the cylinder) and whose reference configuration evolves on longer time scales, leading to an irreversible (plasticlike) behavior. The beauty of the inversion phenomenon is that it relies on the nonlinear anisotropic response of the system and leads to two apparent nonintuitive behaviors: First, the fibers tend to align with the axis, independently of the rotation; second, right-handed helical fibers can lead to both clockwise and counterclockwise rotation depending on the angle and level of precompression.

This publication is based in part upon work supported by the National Science Foundation under Grant No. DMS-0907773 and by Grant No. KUK-C1-013-04, made by King Abdullah University of Science and Technology (KAUST) (A. G.). A. G. is supported through a Wolfson/Royal Society Merit Award.

[1] J.-B. Carnoy, Bull. Soc. R. Bot. Belg. **9**, 157 (1870).
[2] R. Cohen and M. Delbrück, J. Gen. Physiol. **42**, 677 (1959).
[3] K. Bergman *et al.*, Bacteriol. Rev. **33**, 99 (1969).
[4] K. W. Foster and E. Lipson, J. Gen. Microbiol. **62**, 590 (1973).
[5] P. Galland, H. Finger, and Y. Wallacher, J. Plant Physiol. **161**, 733 (2004).
[6] D. Johnson and R. Gamow, Plant Physiol. **49**, 898 (1972).
[7] W. Astbury and R. Preston, Proc. R. Soc. B **129**, 54 (1940).
[8] K. Schulgasser and A. Witztum, Wood Sci. Tech. **41**, 133 (2006).
[9] T. I. Baskin, Annu. Rev. Cell Dev. Biol. **21**, 203 (2005).
[10] M. Middlebrook and R. Preston, Biochim. Biophys. Acta, Biomembr. **9**, 32 (1952).
[11] P. Roelofsen and A. Houwink, Acta Botanica Neerl. **2**, 218 (1953).
[12] E. Castle, Am. J. Bot. **29**, 664 (1942).
[13] J. Ortega, G. Lesh-Laurie, M. Espinosa, E. Ortega, S. Manos, M. Cunning, and J. Olson, Planta **216**, 716 (2003).
[14] J. Ortega and R. Gamow, J. Theor. Biol. **47**, 317 (1974).
[15] M. Wold and R. Gamow, J. Theor. Biol. **159**, 39 (1992).
[16] P. Roelofsen, Adv. Bot. Res. **2**, 69 (1966).
[17] H. Demirkoparan and T. J. Pence, J. Elast. **92**, 61 (2007).
[18] R. Cohen and M. Delbrück, J. Cell. Comp. Physiol. **52**, 361 (1958).